Sereda Borys[1], Doctor of Technical Sciences, Professor, Head Department of Automobiles and Automotive Industry
Середа Б.П., доктор технічних наук, професор, завідувач кафедри автомобілів та автомобільне господарство
ORCID: 0000-0002-9518-381X
e-mail: seredabp@ukr.net

Baskevych Oleksandr[2], Candidate of Physico-mathematical Sciences, Senior Researcher in the Research Unit
Баскевич О.С., кандидат фізико-математичних наук, старший науковий співробітник НДЧ
ORCID: 0000-0002-3227-5637
e-mail: abaskevich@ukr.net

Frolova Liliia[2], Doctor of Technical Sciences, Professor Department of Technology of inorganics and ecology
Фролова Л.А., доктор технічних наук, профессор кафедри технології неорганічних речовин та екології
ORCID: 0000-0001-7970-2264
e-mail: domosedi@i.ua

Kruglyak Irina[1], Doctor of Technical Sciences, Professor, Head Department of industrial engineering
Кругляк І.В., доктор технічних наук, професор, завідувач кафедри галузевого машинобудування
ORCID: 0000-0002-9518-381X
e-mail: krugly@ukr.net

Sereda Dmytro[1], Candidate of Technical Sciences, Associate Professor, Department of industrial engineering
Середа Д.Б., кандидат технічних наук, доцент кафедри галузевого машинобудування господарство
ORCID: 0000-0003-4353-1365
e-mail: seredabp@ukr.net

[1]Dnipro State Technical University, Kamianske
Дніпровський державний технічний університет, м. Кам'янське
[2]Ukrainian State University of Chemistry and Technology, Dnipro
Український державний хіміко-технологічний університет, м. Дніпро

QUANTUM MECHANICAL MODELING OF THE STRUCTURE OF COMPLEX FERRITES

КВАНТОВО-МЕХАНІЧНЕ МОДЕЛЮВАННЯ СТРУКТУРИ СКЛАДНИХ ФЕРИТІВ

We develop a method for the quantum mechanical modeling of the main characteristics of chemical bonds of complex ferrites. The structural characteristics of ferrites were modeled to determine the effect of divalent metal ions on the chemical bonds of oxysene, which is responsible for the formation of a cubic face-centered lattice. The regularity of the lattice parameters change with the number of divalent metals that form the structure of complex ferrites was established.

Keywords: quantum mechanical model, complex ferrites, low-temperature plasma, Schrödinger equation, structure modeling.

Розроблена методика кантово-механічного моделювання основних характеристик хімічних зв'язків складних феритів. Проведено моделювання структурних характеристик феритів з метою встановлення впливу іонів двохвалентних металів на хімічні зв'язки оксисену, який відповідає за утворення кубічної гранецентрованої решітки. Встановлена закономірність зміни параметрів решітки від номеру двохвалентних металів, які утворюють структуру складних феритів.

Ключові слова*: квантово-механічна модель, складні ферити, низькотемпературна плазма, рівняння Шредингера, моделювання структури.*

Development of new promising materials with predictable physical and chemical properties is one of the most urgent tasks of modern science and technology. In this work, we have carried out quantum mechanical modeling of the structural characteristics of ferrites obtained by low-temperature plasma to determine the effect of divalent metal ions on the chemical bonds of oxysene, which is responsible for the formation of a cubic face-centered lattice. For this purpose, a mathematical apparatus for solving the Schrödinger equation in ellipsoidal coordinates was developed. The use of the Coulomb potential and the Yukawa potential is due to the fact that they are separable in ellipsoidal coordinates, and thus the solution of the Schrödinger equation can be reduced to the solution of the Whittaker equation, which is the best result from a physical point of view. The latter equation has half-integer solutions, which means that it is possible to take into account the state of spins that have half-integer values. The following problems have been solved: electron motion in the field of two Coulomb centers, energy of electron-electron interaction, influence of the third Coulomb center on chemical bonding, reduction of the Yukawa potential to the solution of the problem of electron motion in the field of two Coulomb centers. Quantum-mechanical calculations of the energies of chemical bonds of oxygen, taking into account all interactions, as a basis for determining the parameters of the crystal lattice showed a good agreement between experimental and theoretical calculations.

Problem's Formulation

Modern scientific research is aimed at creating new promising materials with predictable properties. The production of nanostructured and nanodispersed ferrites with different electronic structure, physicochemical and electromagnetic properties is a primary goal of modern science [1—4]. The use of nanostructured ferrites in photocatalytic processes allows for the efficient oxidation of organic compounds that do not decompose naturally by biochemical methods and the purification of aqueous solutions is considered the most promising way. Thus, nanoscale ferrites are of considerable practical and scientific interest due to their significant advantages over macroscopic analogs and certainly have great prospects for obtaining new materials based on them.

Analysis of recent research and publications

An analysis of the current literature has shown that ferrites and nanomaterials based on them have enormous potential for use in environmental protection (adsorbents, photocatalysts), as pigments, catalysts, magnets, in the production of galvanic cells and other areas of modern technology. According to numerous experimental and theoretical studies, adsorption materials based on nanoscale ferrites have a large specific surface area, high capacity, fast kinetics, and specific magnetic properties [5—7].

The ability to control the size and shape of ferrite particles makes it possible to obtain materials with predictable mechanical, chemical, magnetic, and electronic properties. The final properties and characteristics of the materials obtained are determined by the technology of particle production and the conditions of their production. Various methods of synthesis make it possible to obtain ferrite particles in the form of nanostructured powders or in the form of nanostructures of various morphologies (nanorods, nanowires, nanotapes, nanotubes, nanospheres, nanocubes, nanosheets, nanolayers, etc.) [8—10].

Using various kinds of physical fields and electric discharges makes it possible to carry out the processes of obtaining oxide-hydroxide compounds at much lower energy costs due to the complex action of many factors accompanying their appearance (UV radiation, radiolysis, etc.) [11].

The use of low-temperature plasma to produce ferrite oxide compounds from aqueous solutions of their salts has been studied for a number of years. There is no complete explanation of the mechanism of a number of phenomena yet, despite the large amount of information obtained. In addition,

the application of glow discharge is mostly related to wastewater treatment, removal of various impurities, or solid-phase reactions. Works have been published on this issue, the study of which allows us to draw certain conclusions [12].

Plasma technologies for the production of ferrites can be considered one of the most promising ways to produce ferrites. Numerous studies have shown that the main influencing factors for hydro-phase technologies are the composition of the initial mixture, the pH of the initial ash, and the parameters of the plasma discharge. When considering the effect of pH on the phase formation of magnetite, nickel and manganese ferrites, it was found that this is the most important parameter that affects the phase composition of the final products. In some works, the acidity of the initial solution is considered as a parameter for controlling the phase composition of ferrites in solvothermal and hydrothermal technologies [13, 14].

Materials and research methods

During the experiments, the corresponding 0.5M solutions of manganese, cobalt, ferrum, and nickel sulfates of different concentrations were used. Ferrites were obtained under the influence of low-temperature plasma. In the course of the experiments, the corresponding 0.5M solutions of manganese, cobalt, ferrum, and nickel sulfates of various concentrations were used. Ferrites were obtained under the influence of low-temperature plasma. After the treatment, the obtained precipitates were washed and dried for further study. Investigation of the phase composition and structural characteristics of the obtained samples was carried out using an X-ray diffractometer DRON-3.0 in monochromatic Co-K_α radiation

Formulation of the study purpose

Obtained experimental results do not provide an explanation of the trends in the structures of ferrites. Therefore, it is necessary to establish the mechanism of structural changes in manganese, ferrite, sobalt, and nickel ferrites using the quantum mechanics apparatus.

Presenting main material

Low-temperature plasma is characterized by temperatures of up to 10,000 K and fully or partially ionized atoms and molecules of the materials under study.

Glow discharge was used to produce complex ferrites. Fig. 1 shows the discharge scheme over an electrolytic cathode (the surface of a solution of complex ferrites salts):
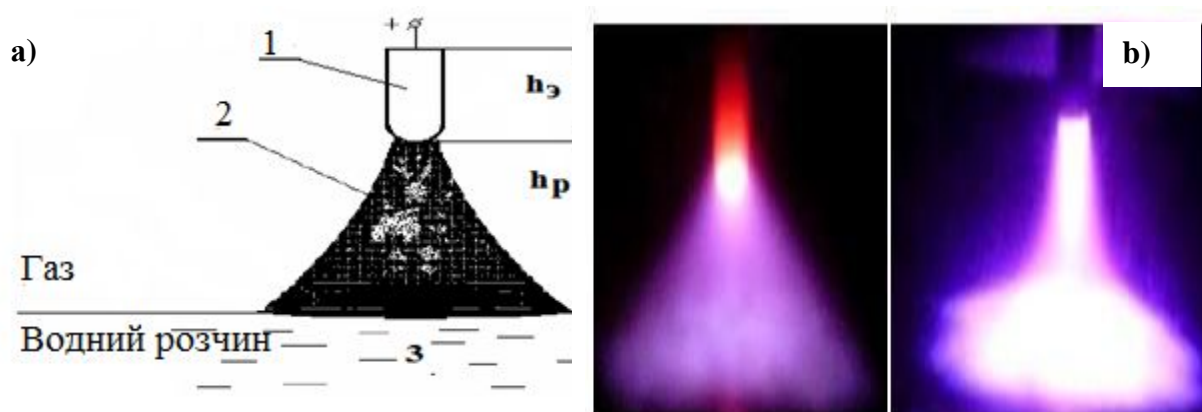
Fig. 1. Stationary discharge over an electrolyte cathode: schematic image (a), discharge of a contact non-equilibrium plasma observed in a plasma-chemical reactor during the treatment of aqueous solutions of ferrite salts (b). 1 — electrode, 2 — plasma discharge, 3 — aqueous electrolyte electrode

Thus, Fig. 1 shows that ferrite formation occurs in a rather thin layer of plasma above the surface of the aqueous solution (reaction zone). The interaction between low-temperature plasma particles is determined by significant short-range forces that appear during their collisions and a significant temperature difference. We will assume that the previous collisions and interactions do not affect the subsequent ones. The Yukawa potential is the most appropriate for this type of interaction, since it

is shorter than the Coulomb potential. And the electrostatic Coulomb interaction has a significant interaction radius for low temperatures.

To build a physical model of chemical bonding, the potential energy of atomic interaction will be defined as a function of the charges of the nuclei of atoms Z_a and Z_b and the distances between them — r ("field of central forces"). The potential functions of short-range forces (Yukawa potential) can be written as:

$$V_{Юкави} = \frac{Z_a Z_b}{r} e^{-\beta r} \qquad (1)$$

β — shielding factor that shows how the electric charge of atoms changes

$$\beta = \frac{Z_a^{2/3} + Z_b^{2/3}}{a_0} \qquad (2)$$

a_0 — boriv radius.

If in an ideal state the charges of nuclei are integer, then as these charges surround electrons and ions, the effective charges decrease and become decimal. In the state of low-temperature plasma, charged particles can be neutral, charged, ionized, and in different quantum states characterized by various spins s ($s = \frac{1}{2}, s = \frac{3}{2}, s = \frac{5}{2} \cdots$). We will develop a formalism for the transition from the Yukawa potential to the Coulomb potential in the ellipsoidal coordinate system. Within the framework of the face-centered cubic structure of iron spinels, it has been established that the basis for calculating the parameters of the crystal lattice is the chemical bonds of oxygen O=O, in the octahedra of which trivalent iron atoms are embedded. To determine the influence of divalent metals of the iron group on the crystal lattice parameter, it is necessary to take into account all interactions that affect the O=O chemical bond. In this case, the formation of the ferrite structure begins at a low-temperature plasma temperature of about 10000 K. At this temperature, all atoms are in full or partial ionization. When the plasma cools, chemical bonds are formed, and then structures with minimal energy. Initially, octahedra and tetrahedra with minimum formation energies are formed. We will consider the O=O chemical bond as the basis for determining the parameters of crystal lattices, and the influence of other atoms and chemical bonds as the electrostatic effect of the sum of third centers on this bond and on the bond energy.

We will consider the further completion of the structure as the addition of tetrahedra with divalent atoms that affect the chemical bonds in the form of third charged centers. For these calculations, it is necessary to perform a series of quantum mechanical calculations that would take into account all these interactions. We will use the Schrödinger equation for an electron in the field of two Coulomb centers, which has the following form [15—18]:

$$\Delta \Psi + 2[E + U(r_a, r_b)]\Psi = 0, \qquad (3)$$

where $U(r_a, r_b)$ — potential energy operator, Δ — Laplace operator in ellipsoidal coordinate systems, which is expressed using the Lamé coefficients (1):

$$\Delta = \left\{ \frac{4}{R^2(\lambda^2 + \mu^2)} \left[\frac{\partial}{\partial \lambda}(\lambda^2 - 1)\frac{\partial}{\partial \lambda} + \frac{\partial}{\partial \mu}(1 - \mu^2)\frac{\partial}{\partial \mu} \right] + \frac{4}{R^2(\lambda^2 - 1)(1 - \mu^2)}\frac{\partial^2}{\partial \varphi^2} \right\},$$

where r_a і r_b — distance from the electron to the centers A and B. Denote by R the distance between the potential centers, then equation (3) in ellipsoidal coordinates will be:

$$\left\{ \frac{4}{R^2(\lambda^2 + \mu^2)} \left[\frac{\partial}{\partial \lambda}(\lambda^2 - 1)\frac{\partial}{\partial \lambda} + \frac{\partial}{\partial \mu}(1 - \mu^2)\frac{\partial}{\partial \mu} \right] + \frac{4}{R^2(\lambda^2 - 1)(1 - \mu^2)}\frac{\partial^2}{\partial \varphi^2} \right\}\Psi + 2[E + U(\lambda, \mu)]\Psi = 0, \qquad (4)$$

where E — electron energy.

The choice of an ellipsoidal coordinate system is due to the fact that the Coulomb and Yukawa potentials are separable in them. To solve equation (4), it is necessary that the variables λ and μ in the potential functions to be separated and the condition:

$$U(\lambda,\mu)(\lambda^2 - \mu^2) = \varphi_1(\lambda) - \varphi_2(\mu),$$

This class of separate functions includes functions of the type:

$$U(\lambda,\mu) = \frac{F_1(\lambda,\mu)}{\lambda - \mu} + \frac{F_2(\lambda,\mu)}{\lambda + \mu}, \tag{5}$$

where $F_1(\lambda,\mu) = f_1(\lambda) + f_2(\mu)$; $F_2(\lambda,\mu) = f_1(\lambda) - f_2(\mu)$.

Expression (5) can be rewritten in the following form:

$$U(\lambda,\mu) = \frac{\Phi_1(\lambda,\mu)}{\lambda^2 - \mu^2} + \frac{\Phi_2(\lambda,\mu)}{\lambda^2 + \mu^2}.$$

For the Coulomb potential, we present the solution of equation (3), which is divided into three ordinary differential equations of the second order [16,17]:

$$\left[\frac{\partial^2}{\partial \varphi^2} + \Lambda^2 \right] \Phi(\varphi) = 0; \tag{6}$$

$$\left[\frac{\partial}{\partial \mu}(1 - \mu^2)\frac{\partial}{\partial \mu} + \frac{\Lambda^2}{1 - \mu^2} - \mu^2 \varepsilon + \mu Z^+ + A \right] Y(\mu) = 0; \tag{7}$$

$$\left[\frac{\partial}{\partial \lambda}(\lambda^2 - 1)\frac{\partial}{\partial \lambda} - \frac{\Lambda^2}{\lambda^2 - 1} + \lambda^2 \varepsilon + \lambda Z^+ - A \right] X(\lambda) = 0, \tag{8}$$

where $\Phi(\varphi) = \exp(i\Lambda\varphi)$, $|\Lambda|$ — integer.

$\varepsilon = \dfrac{ER^2}{2}$; $Z^{(\pm)} = (Z_a \pm Z_b)R / \beta$; $A(R)$ — permanent separation.

Calculate some states using the formula:

$$E_{k,\Lambda,n} = \frac{\left\langle \Psi_{k,\Lambda,n} \middle| H_0 \middle| \Psi_{k,\Lambda,n}^* \right\rangle}{\left\langle \Psi_{k,\Lambda,n} \middle| \Psi_{k,\Lambda,n}^* \right\rangle},$$

where H_0 — hamiltonian of the two-center problem, k, Λ, n — quantum numbers:

$$\ddot{H} = \sum_{i=1}^{\infty} \left(-\frac{1}{2}\Delta_i - \frac{Z}{r_i} \right) + \frac{1}{r_{12}}.$$

$\Psi_{k,\Lambda,n}$, $\Psi_{k,\Lambda,n}^*$ — wave functions that are the solution to the Whittaker equation [17]:

$$E_{\frac{1}{2},0,0} = \frac{4\left[\frac{1}{2}(b_1 - Z^+) + e^{4b_1} E_i(-4b_1)(b^2 - b_1 Z^+ - \frac{1}{4}b_1) \right]}{R^2 \left[\frac{1}{2b_1} - \frac{4}{3}b_1 e^{4b_1} E_i(-4b_1) \right]}; \tag{9}$$

$$E_{\frac{3}{2},0,0} = \frac{1}{R^2 \left[\frac{1}{2b_3} - 4b_3 - 16b_3^2 - 4b_3(1 + 4b_3)^2 e^{4b_3} E_i(-4b_3) \right]} \times$$

$$\times 12\left\{ \left(\left(\frac{3b_3}{4} - Z^+\left(\frac{1}{2} + b_3 + 4b_3 \right) - e^{4b_3} E_i(-4b_3) \right) * \left[\frac{1}{4}b_3 + b_3^2 - 4b_3^2 + Z^+(16b_3^3 + 8b_3^2 + b_3) \right] \right) \right\}. \tag{10}$$

Let us limit ourselves to the spin s=3/2. If a chemical bond has more than one electron, then electron-electron interactions must be taken into account. We calculate electron-electron interactions using the Slater determinant [17]:

$$\Psi_{det} = \begin{vmatrix} u_1(1) & u_2(1) \\ u_2(2) & u_2(2) \end{vmatrix}, \tag{11}$$

here $u_1 = \alpha_0 \varphi^{(mod)}$; $u_2 = \beta_0 \varphi^{(mod)}$, that is, the model two-center field functions were used as the basis H_2^+, $\dfrac{1}{r_{1,2}}$ can be represented as a Neumann expansion [17]:

$$W_1(\lambda, \mu, \varphi, Z_3) = \frac{2}{R} \sum_{p=0}^{\infty} \sum_{m=-p}^{p} (-1)^m (2p+1) \left[\frac{(p-|m|)!}{(p+|m|)!} \right] P_p^{|m|}(\lambda_<) Q_p^{|m|}(\lambda_>) P_p^{|m|}(\mu_3) Q_p^{|m|}(\mu_3) e^{im(\varphi - \varphi_3)}, \tag{12}$$

where $\lambda_3 = \dfrac{R_2 + R_3}{R_1}$; $\mu_3 = \dfrac{R_2 - R_3}{R_1}$; $\lambda_{\substack{< \\ >}}$ — higher or lower of the values of; $P_p^{|m|}(\lambda_<)$ і $Q_p^{|m|}(\lambda_>)$ attached Legendre functions of the I and II kind.

$$E_{e-e} = \left\langle \psi_{det} \left| \frac{1}{r_{1,2}} \right| \psi_{det}^* \right\rangle = \frac{4}{R \left[\dfrac{1}{2a} - \dfrac{4}{3} a \cdot e^{4a} \cdot E_i(-4a) \right]^2} *$$

$$\left[\left(\frac{3}{40a^2} + \frac{1}{20a^2} \right) \cdot (C + \ln 2a) + e^{8a} E_i^2(-8a) \left(\frac{3}{40a^2} + \frac{11}{20a} + \frac{7}{5} + \frac{8a}{15} \right) + e^{4a} E_i^2(-8a) \frac{4a^2}{15} + \right.$$

$$\left. + e^{4a} E_i^2(-4a) \left(-\frac{3}{20a^2} + \frac{1}{2a} - \frac{1}{5} \right) + \frac{1}{8a} - \frac{1}{10} \right].$$

Let us assume elementary acts of chemical reactions as the interaction of chemical bonds with positive and negative charges. We will consider these charges as the influence of the third Coulomb center on a separately selected chemical bond. Let's imagine the third Coulomb center as a certain perturbation acting on a chemical bond. Then the Hamiltonian of the three-center system can be represented as:

$$H_0 = -\frac{h^2}{2M_1} \Delta \vec{R}_1 - \frac{h^2}{2M_2} \Delta \vec{R}_2 - \frac{h^2}{2M_3} \Delta \vec{R}_3 + \frac{Z_1 Z_2}{|\vec{R}_2 - \vec{R}_1|} + \frac{Z_1 Z_3}{|\vec{R}_3 - \vec{R}_1|} + \frac{Z_3 Z_2}{|\vec{R}_3 - \vec{R}_2|}, \tag{13}$$

H_0 — Hamiltonian of the interaction of three particles. Let's enter the Jacobi coordinates:

$$\vec{R} = \frac{M_1 \vec{R}_1 + M_2 \vec{R}_2 + M_3 \vec{R}_3}{M_1 + M_2 + M_3}, \quad r = R_3 - \frac{M_1 \vec{R}_1 + M_2 \vec{R}_2}{M_1 + M_2}, \quad \vec{R} = \vec{R}_2 - \vec{R}_1,$$

$$H_0 = -\frac{h^2}{2M_t} \Delta \vec{R} - \frac{h^2}{2M} \Delta \vec{R} - \frac{h^2}{2M} \Delta \vec{r} + \frac{Z_1 Z_2}{R} + \frac{Z_1 Z_3}{r_1} + \frac{Z_2 Z_3}{r_2}, \tag{14}$$

where the following notations are entered:

$$M_t = M_1 + M_2 + M_3, \quad \frac{1}{M} = \frac{1}{M_1} + \frac{1}{M_2}.$$

Taking these assumptions into account, we will choose two Coulomb centers as a basis, and represent the perturbation caused by the influence of the third center in the form of a Neumann expansion [15]:

$$W_3 = \frac{2Z_3}{R} \sum_{p=0}^{\infty} \sum_{m=-p}^{p} (-1)^m (2p+1) \left[\frac{(p-|m|)!}{(p+|m|)!} \right] P_p^{|m|}(\lambda_<) Q_p^{|m|}(\lambda_>) P_p^{|m|}(\mu_3) Q_p^{|m|}(\mu_3) e^{im(\varphi - \varphi_3)}. \tag{15}$$

where $\lambda_3 = \dfrac{R_2 + R_3}{R_1}$, $\mu_3 = \dfrac{R_2 - R_3}{R_1}$, $\lambda_{\substack{< \\ >}}$ — higher or lower of the values of, $P_p^{|m|}(\lambda_<)$ і $Q_p^{|m|}(\lambda_>)$ attached Legendre functions of the I and II kind.

Then taking into consideration the perturbation, the energy of the three-part problem will be:

$$W_3 = \frac{\left\langle \Psi \left| H + W_{\frac{1}{2},0,0} \right| \Psi^* \right\rangle}{\left\langle \Psi \middle| \Psi^* \right\rangle} = E_0(R_1) +$$

$$+ \sum_{i=1}^{N} \frac{4aZ_i}{R_i \left[\frac{1}{2a} - \frac{4a}{3} e^{4a} E_i(-4a) \right]} \left\{ Q_0^0(\lambda_3) \left[\frac{2}{3} e^{4a} E_i(-4a) - \frac{1}{4a^2} \right] - \frac{1}{8a^2 e^{2a(\lambda_3-1)}} \left[P_2(\lambda_3) P_2(\mu_3) - 1 \right] \cdot$$

$$\cdot \left[e^{2a(\lambda_3+1)} E_i(-2a(\lambda_3+1) - e^{2a(\lambda_3-1)} E_i(-2a(\lambda_3-1)) \right] - Q_2(\lambda_3) P(\mu_3) \left[\frac{2}{3} e^{4a} E_i(-4a) + \right.$$

$$+ (\lambda_3^2 - 1) e^{2a(\lambda_3-1)} E_i(-2a(\lambda_3-1)) + e^{-2a(\lambda_3-1)} \left(\frac{1}{2a} - \frac{1}{4a^2} - \frac{\lambda_3}{2a} \right) + \frac{1}{4a^2} \right] +$$

$$+ Q_0(\lambda_3) P_2(\lambda_3) P_2(\mu_3) \left[(\lambda_3^2 - 1) e^{2a(\lambda_3+1)} E_i(-2a(\lambda_3+1)) - \left(\frac{1}{2a} - \frac{1}{4a^2} - \frac{\lambda_3}{2a} \right) \right] e^{-2a(\lambda_3-1)} \cdot$$

$$\cdot P_2(\lambda_3) P_2(\mu_3) \cdot \left[e^{4a} E_i(\lambda_3+1) E_i(-2a(\lambda_3+1)) + \frac{1}{2a} e^{-2a(\lambda_3} - 1) \right] \right\}.$$

$$\Delta W_{\frac{3}{2},0,0} = \Delta W_{\frac{1}{2},0,0} + \frac{2Z_i}{R} \left\{ \left[2Q_o(\lambda_3) - \frac{9}{4} P_2(\lambda_3) \right] * \left[\left(\frac{1}{a} + \frac{1}{2a^2} + \frac{1}{3} \right) - \frac{8a}{3}(1+a) e^{4a} E_i(-4a) - \right. \right.$$

$$- 2a\lambda_3^3 + (2a-1)\lambda_3^2 + \frac{2a}{3} + \frac{3}{4a^2} + \frac{4}{3} + \frac{8a(1+a)}{3} e^{4a} E_i(-2a(\lambda_3-1)) \right] + \left[1 - \frac{9}{4} P_2(\mu_3) P_2(\lambda_3) \right] *$$

$$* \left[2Q_0(\lambda_3) e^{-2a(\lambda_3-1)} \left(2a\lambda_3^3 + (1-2a)\lambda_3^2 + \lambda_3 \left(\frac{1}{a} + \frac{4a}{3} \right) - \frac{2}{3} - \frac{4a}{3} - \frac{3}{4a^2} \right) + \right.$$

$$+ e^{4a} E_i(2a(\lambda_3+1)) \cdot \left(\frac{28a}{3} - 6 + \frac{10}{a} - \frac{5}{4a^2} \right) + \frac{4a}{3}(1+a) e^{4a} E(-2a(\lambda_3+1)) +$$

$$+ \frac{4a}{3}(1+a) \left[e^{4a} E_i(-2a(\lambda_3-1)) \cdot (\lambda_3+1) - e^{4a} E_i(-2a(\lambda_3+1)) \cdot (\lambda_3-1) \right] \right] +$$

$$+ \frac{9}{4} P_2(\mu_3) P_2(\lambda_3) \left[2a\lambda_3^4 + 4\lambda_3^3(1-a) + \lambda_3^2 \left(\frac{3}{a} - 1 + \frac{4a}{3} \right) + \lambda_3 \left(\frac{3}{a^2} - \frac{1}{a} - \frac{4a}{3} + \frac{4}{3} \right) + \frac{4a}{3} - \frac{4}{3} - \frac{3}{4a^2} + \right.$$

$$+ \frac{3}{a^2} + \frac{8a}{3} e^{4a}(1+a) E_i^2(-2a(\lambda_3-1)) \right]. \tag{16}$$

Thus, there are two terms in formula (16): the binding energy of the O=O molecule and the term representing the influence of the third Coulomb center on the chemical bond of this molecule.

Let us consider the motion of an electron in the field of two centers that have a Yukawa-type potential:

$$V(r_a, r_b) = Z_1 \frac{e^{-\beta r_a}}{r_a} + Z_2 \frac{e^{-\beta r_b}}{r_b}. \tag{17}$$

Then in the ellipsoidal coordinate system:

$$V(\lambda, \mu) = Z_1 \frac{e^{-\beta R_a (\lambda + \mu)/2}}{\lambda + \mu} + Z_2 \frac{e^{-\beta R_a (\lambda - \mu)/2}}{\lambda - \mu}. \tag{18}$$

Let's expand the exponent in the numerator into a series $e = 1 - x + ...$
After simple transformations, we get the following:

$$V(\lambda, \mu) = \frac{2}{R}\left(\frac{Z_1}{\lambda + \mu} + \frac{Z_2}{\lambda - \mu}\right) + Z^+ \sum_{i=1}^{\infty} (-1)^i \frac{\beta^i R^{i-1}}{i!} \lambda^{i-1} + Z^- \sum_{i=2}^{\infty} (-1)^i \frac{\beta^i R^{i-1}}{i!} \lambda^{i-1} +$$

$$+ Z^+ \sum_{j=0}^{\infty} \sum_{i=0}^{\infty} (-1)^{i+j-1} \frac{\beta^{i+2j} R^{i+j}}{(8 + 32(i+j-4))} \lambda^{i-3} \mu^{2i+2j}.$$

The last expression can be represented as:

$$V(\lambda, \mu) = \frac{2}{R}\left(\frac{Z_1}{\lambda + \mu} + \frac{Z_2}{\lambda - \mu}\right) + \Delta W_{Юкави}.$$

where $\Delta W_{Юкави}$ — represents the addition of the Yukawa potential to the Coulomb potential.

$$\Delta W_{Юкави} = Z^+ \sum_{i=1}^{\infty} (-1)^i \frac{\alpha^i R^{i-1}}{i!}\left[2I_{i+1} + 2E_i(-4a)/3\right] + Z^- \sum_{i=2}^{\infty} (-1)^i \frac{\alpha^i R^{i-1}}{i!}\left[2I_2 + 2E_i(-4a)/(i+2)\right] +$$

$$+ Z^+ \sum_{j=0}^{\infty} \sum_{i=0}^{\infty} (-1)^{i+j-1} \frac{\alpha^{i+2j} R^{i+j}}{(8 + 32(i+j-4))}\left[\frac{2I_{i-1}}{(2(i+j)+1)} + \frac{2E_i(-4a)}{(2(i+j)+3)}\right]. \tag{19}$$

To calculate the binding energy of molecules, use the expression:

$$E_{O=O} = 2E_{\frac{1}{2},0,0} + E_{ee} + \sum (W_3 + \Delta W_{Юкави}). \tag{20}$$
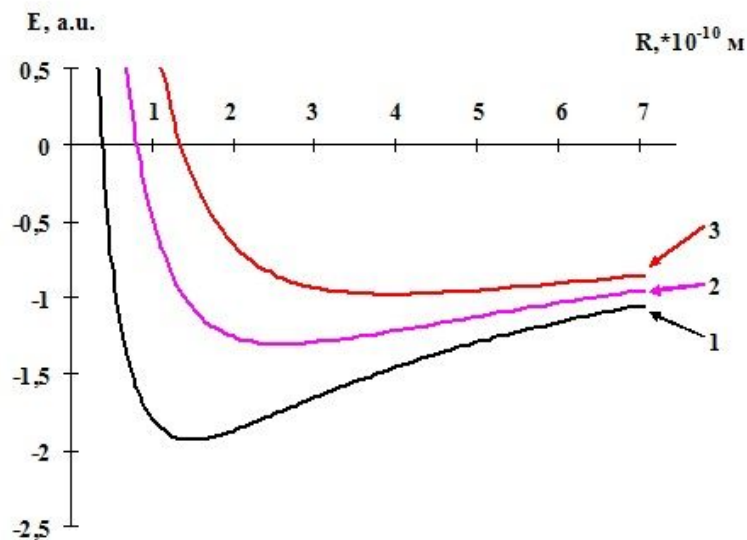
Fig. 2. The chemical bonding energy of an oxygen molecule in states (a.u. atomic units): 1 — in condition $s = \frac{1}{2}$, 2 — $s = \frac{3}{2}$, 3 — $s = \frac{5}{2}$

Let's calculate the binding energy of the oxygen molecule using formula (20) Fig. 2. Curve 1 was calculated using the formulas for the Coulomb potential, and curves 2 and 3 were calculated taking into account the Yukawa potential. The calculation of curve 1 showed that in the ground state, the interatomic distance and binding energy coincide with the experimental data (0.189 a.u.) to within 2%. Curves 2 and 3 show that the chemical bond "falls apart" with increasing temperature (spin in the 3/2

and 5/2 states are equivalent to high temperatures). Using this method, we calculated the effect on the chemical bond of the divalent atoms of the cubic structure of manganese, cobalt, ferrum, and nickel, which are located in the centers of tetrahedra (Fig. 3) and significantly affect octahedra with trivalent ferrum atoms, and therefore affect the chemical bond of oxygen. Quantum mechanical calculations have shown that with increasing atomic number, the binding energy increases and the interatomic distance O=O decreases, which corresponds to the experimental and tabulated values of the crystal lattice parameters (Fig. 4), (Tabl. 1) [19].
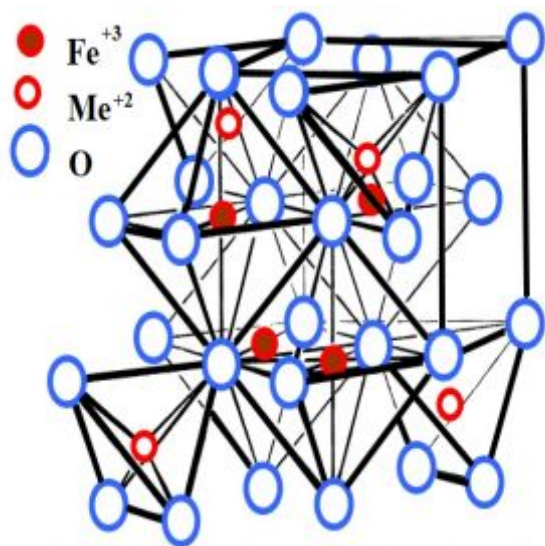
Fig. 3. Structural forms of ferrites. Me^{+2} — metal ions of manganese, cobalt, ferrum and nickel
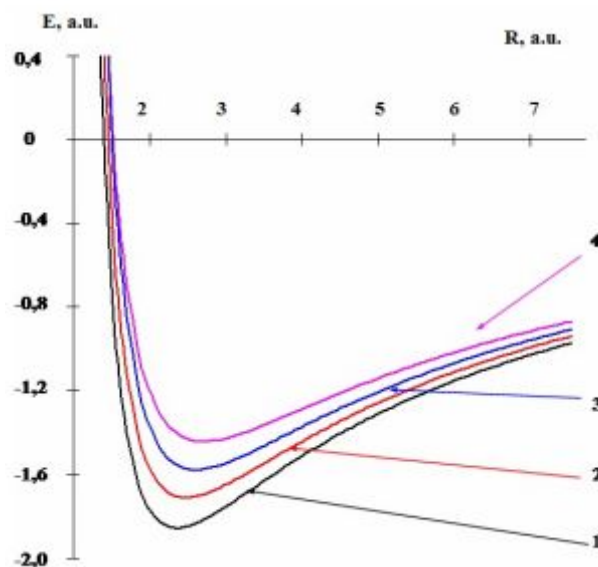
Fig. 4. Binding energies of 1— Nicotine, 2— Cobalt, 3— Ferric, 4— Manganese

Table 1. Calculation of crystal lattice parameters of stoichiometric ferrites

Composition of ferrite	Table value of the crystal lattice parameter, a, nm	Calculated value of the crystal lattice parameter a, nm	The value of the binding energy of the oxygen molecule in the structures of ferrites, a.e.	Interatomic distance in the oxygen molecule R, a.u.
$MnFe_2O_4$	0,8515	0,8518	0,1354	2,2262
$FeFe_2O_4$	0,8397	0,8390	0,1531	2,1865
$CoFe_2O_4$	0,8777	0,8385	0,1642	2,1811
$NiFe_2O_4$	0,8337	0,8339	0,1805	2,1680

Conclusions

We performed the quantum mechanical modeling of energies and interatomic distances to show the regularities of ferrite structure formation. With an increase in the atomic number, the binding energy increases and the interatomic distance O=O decreases, which corresponds to the experimental and tabulated values of the crystal lattice parameters. Establishing the regularities of ferrite structure formation will make it possible to find out the conditions for creating new varieties of ferrite, and thus to create new materials with unique properties. This method of quantum mechanical calculations can be used to calculate the binding energy of a wide range of chemical compounds.

References

[1]   Dastjerdi O. D., Shokrollahi H., Mirshekari S. A. (2023). Review of synthesis, characterization, and magnetic properties of soft spinel ferrites. *Inorganic Chemistry Communications*, [in English]

[2]   Thakur A., Vermo R., Wan F., Ravelo B. et al.(2023). Investigation of structural, elastic and magnetic properties of Cu2+ ions substituted cobalt nano ferrites. *Journal of Magnetism and Magnetic Materials.* Vol. 581, [in English]

[3]   Ludhiya V., Haricumar N., Ravinder D., Edukondalu A. (2023). Structural, optical, dielectric and magnetic properties of Nd3+ ion substituted Ni-Mg-Cu spinel ferrites. Inorganic Chemistry Communications. Vol. 150, [in English]

[4]   Mondal N. J., Sonkar R., Boro B., Ghosh M.P. (2023). Nanocrystalline Ni–Zn spinel ferrites: size-dependent physical, photocatalytic and antioxidant properties. *Nanoscale Advances*, Vol. 5, №. 20 [in English]

[5]   Kumari S., Sharma R., Thacur N., Kumari A. (2023). Removal of organic and inorganic effluents from wastewater by using degradation and adsorption properties of transition metal-doped nickel ferrite. *Environmental Science and Pollution Research* [in English]

[6]   Sulaiman N. I., Abu Bakar N. H. H., Abu Bakar M. (2024). Effect of Al-Doping on Structural and Adsorption Properties of NiFe2O4 via Modified Sol–Gel Approach for CO2 Adsorption. *Chemistry Africa.* [in English]

[7]   Ma Y., Vang., Gao C., Yan R.(2023). Carbon nanotube-loaded copper-nickel ferrite activated persulfate system for adsorption and degradation of oxytetracycline hydrochloride. *Journal of Colloid and Interface Science*, Vol. 640 [in English]

[8]   Gavilan H., Rizzo G.M.R, Silvestri N., Mai B.T. et al. (2023). Scale-up approach for the preparation of magnetic ferrite nanocubes and other shapes with benchmark performance for magnetic hyperthermia applications. *Nature Protocols*, Vol. 18, №. 3 [in English]

[9]   Latwal M., Arora S., Bhardwaj R., Panday G. et al. (2023). Synthesis of ferrite nanocubes. *Ferrite Nanostructured Magnetic Materials*, – Woodhead Publishing [in English]

[10] Manisekaran R., Manisekaran R. (2018).Multiple Iterative Seeding of Surface Plasmon Enhanced Cobalt-Iron Oxide Nanokernels for Cancer Theranostics. *Design and Evaluation of Plasmonic/Magnetic Au-MFe2O4 (M-Fe/Co/Mn) Core-Shell Nanoparticles Functionalized with Doxorubicin for Cancer Therapeutics*, [in English]

[11] Reddy M. P., Mohamed A. M. A. (2015).0 One-pot solvothermal synthesis and performance of mesoporous magnetic ferrite MFe2O4 nanospheres. *Microporous and Mesoporous Materials*, Vol. 215 [in English]

[12] Achola L. A., Shubhashish S., Tobin Z., Su Y., et al. (2023). Microwave hydrothermal synthesis of mesoporous first-row transition metal ferrites. *Chemistry of Materials*, Vol. 34, №. 17 [in English]

[13] Frolova L. A., Derimova A. V. (2019). Factors controlling magnetic properties of CoFe2O4 nanoparticles prepared by contact low-temperature non-equilibrium plasma method. *Journal of Chemical Technology and Metallurgy*, Vol. 54, №. 5 [in English]

[14] Saremi A., Mirkazerni S.M., Sazvar A., Rezale H. (2024). Controlling magnetic and surface properties of cobalt ferrite nanoparticles: A comparison of co-precipitation and solvothermal synthesis methods. *Solid State Sciences*, Vol. 148 [in English]

[15] Baskevych O.S., Sobolev V.V., Sereda B.P. (2020). Modeling the influence of shock waves on the stability of chemical links during super-deep penetration of microparticles *Matematychne modeliuvannia*, № 1(42), C.116-124 [in English]

[16] Bereza O.Yu., Filinenko N.Yu,, Baskevych O.S. Rozrakhunok energii khimichnogo zviazku faz, scho Mistiat bor u splavakh systemy Fe-B-C (2012). Naukovi visti natsionalnogo tekhnichnogo universytetu "Kyiivskyi politekhnichnyi instutut", Vol.84, №4, P.116-120. [in Ukrainian]

[17] Sobolev V.V., Baskevych O.S., Varenyk Ye, O. (2015}. Elektrostymuliovani khimichni reaktsii v atmospheri vugilnykh shakht. [Elecricall stimulated chemical reaction in the atmosphere of coal mines]. Monograph.–Kharkiv: Vydavnytstvo "Tekhnologichnyi tsentr". − 80 c. [in Ukrainian]

[18] Sobolev V.V., Bilan N.V., Baskevich A.S, Stefanovich I.I. (2018). Electrical charges as catalysts of chemical reactions on a solid surface. *Naukovyi Visnyk NHU*, №4 [in Ehglish]

[19] PCPDFWIN, Version 2.0, August 1998. Copyright ® 1998. JCPDS−ICDD

Список використаної літератури

1. Dastjerdi O. D., Shokrollahi H., Mirshekari S. A review of synthesis, characterization, and magnetic properties of soft spinel ferrites //Inorganic Chemistry Communications. 2023. C. 110797.

2. Thakur A., Vermo R., Wan F., Ravelo B. et al. Investigation of structural, elastic and magnetic properties of Cu2+ ions substituted cobalt nano ferrites //Journal of Magnetism and Magnetic Materials. 2023. V. 581. C. 170980.

3. Ludhiya V. , Haricumar N.,Ravinder D., Edukondalu A. Structural, optical, dielectric and magnetic properties of Nd3+ ion substituted Ni-Mg-Cu spinel ferrites //Inorganic Chemistry Communications. 2023. V. 150. C. 110558.

4. Mondal N. J., Sonkar R., Boro B., Ghosh M.P. Nanocrystalline Ni–Zn spinel ferrites: size-dependent physical, photocatalytic and antioxidant properties //Nanoscale Advances. 2023. V. 5. №. 20. C. 5460–5475.

5. Kumari S., Sharma R., Thacur N., Kumari A. Removal of organic and inorganic effluents from wastewater by using degradation and adsorption properties of transition metal-doped nickel ferrite //Environmental Science and Pollution Research. 2023. C. 1–20.

6. Sulaiman N. I., Abu Bakar N. H. H., Abu Bakar M. Effect of Al-Doping on Structural and Adsorption Properties of NiFe2O4 via Modified Sol–Gel Approach for CO2 Adsorption //Chemistry Africa. 2024. C. 1–16.

7. Ma Y., Vang., Gao C., Yan R. Carbon nanotube-loaded copper-nickel ferrite activated persulfate system for adsorption and degradation of oxytetracycline hydrochloride //Journal of Colloid and Interface Science. 2023. T. 640. C. 761–774

8. Gavilan H., Rizzo G.M.R, Silvestri N., Mai B.T. et al. Scale-up approach for the preparation of magnetic ferrite nanocubes and other shapes with benchmark performance for magnetic hyperthermia applications //Nature Protocols. 2023. T. 18. №. 3. C. 783–809.

9. Latwal M., Arora S., Bhardwaj R., Panday G. et al. Synthesis of ferrite nanocubes //Ferrite Nanostructured Magnetic Materials. Woodhead Publishing, 2023. C. 375–390.

10. Manisekaran R., Manisekaran R. Multiple Iterative Seeding of Surface Plasmon Enhanced Cobalt-Iron Oxide Nanokernels for Cancer Theranostics //Design and Evaluation of Plasmonic/Magnetic Au-MFe2O4 (M-Fe/Co/Mn) Core-Shell Nanoparticles Functionalized with Doxorubicin for Cancer Therapeutics. 2018. C. 115–138.

11. Reddy M. P., Mohamed A. M. A. One-pot solvothermal synthesis and performance of mesoporous magnetic ferrite MFe2O4 nanospheres //Microporous and Mesoporous Materials. 2015. T. 215. C. 37–45.

12. Achola L. A., Shubhashish S., Tobin Z., Su Y., et al. Microwave hydrothermal synthesis of mesoporous first-row transition metal ferrites //Chemistry of Materials. 2022. T. 34. №. 17. C. 7692–7704.

13. Frolova L. A., Derimova A. V. Factors controlling magnetic properties of CoFe2O4 nanoparticles prepared by contact low-temperature non-equilibrium plasma method //Journal of Chemical Technology and Metallurgy. 2019. T. 54. №. 5. C. 1040–1046.

14. Saremi A., Mirkazerni S.M., Sazvar A., Rezale H. Controlling magnetic and surface properties of cobalt ferrite nanoparticles: A comparison of co-precipitation and solvothermal synthesis methods //Solid State Sciences. 2024. T. 148. C. 107432.

15. Baskevych O.S., Sobolev V.V., Sereda B.P. Modeling the influence of shock waves on the stability of chemical links during super-deep penetration of microparticles / Математичне моделювання. № 1(42). 2020. C. 116−124.

16. Береза О.Ю., Филоненко Н.Ю., Баскевич О.С. Розрахунок енергії хімічного зв'язку фаз, що містять бор у сплавах системи Fe-B-C/ Наукові вісті національного технічного університету України «Київський політехнічний інститут». №4(84). 2012. C. 116−120.

17. Соболєв В.В., О.С. Баскевич, Є.О. Вареник. Електростимульовані хімічні реакції в атмосфері вугільних шахт. Монографія. Харків: видавництво "Технологічний центр", 2015. 80 с.
18. Sobolev V.V., Bilan N.V., Baskevich A.S., Stefanovich I.I. Electrical charges as catalysts of chemical reactions on a solid surface].Naukovyi Visnyk NHU. № 4. 2018. P. 50–58.
19. PCPDFWIN, Version 2.0, August 1998. Copyright ® 1998. JCPDS−ICDD.